2-2014

Radiation modeling in the Earth and Mars atmospheres using LRO/CRaTER with the EMMREM Module

Colin J. Joyce
University of New Hampshire, Colin.Joyce@unh.edu

Nathan A. Schwadron
University of New Hampshire, Nathan.Schwadron@unh.edu

Jody K. Wilson
University of New Hampshire, jody.wilson@unh.edu

Harlan E. Spence
University of New Hampshire, harlan.spence@unh.edu

Justin Kasper
University of Michigan - Ann Arbor

See next page for additional authors

Recommended Citation

Joyce, C. J., et al. (2014), Radiationmodeling in the Earth and Mars atmo-spheres using LRO/CRaTER with theEMMREM Module, Space Weather, 12,112–119, doi:10.1002/2013SW000997.

AGU PUBLICATIONS

Space Weather

RESEARCH ARTICLE

10.1002/2013SW000997

Special Section:
The Crater Special Issue of Space Weather: Building the Observational Foundation to Deduce Biological Effects of Space Radiation

Key Points:
- We model GCR dose and dose equivalent rates in Earth and Mars atmospheres
- Dose rates are in reasonable agreement with nearby measurements
- Data products will soon be made available on PREDICCS website

Correspondence to:
C. J. Joyce,
cjl46@unh.edu

Citation:
Joyce, C. J., et al. (2014), Radiation modeling in the Earth and Mars atmospheres using LRO/CRaTER with the EMMREM Module, *Space Weather*, *12*, 112–119, doi:10.1002/2013SW000997.

Received 1 OCT 2013
Accepted 14 JAN 2014
Accepted article online 17 JAN 2014
Published online 14 FEB 2014

Radiation modeling in the Earth and Mars atmospheres using LRO/CRaTER with the EMMREM Module

C. J. Joyce[1], N. A. Schwadron[1], J. K. Wilson[1], H. E. Spence[1], J. C. Kasper[2], M. Golightly[1], J. B. Blake[3], L. W. Townsend[4], A. W. Case[5], E. Semones[6], S. Smith[1], and C. J. Zeitlin[7]

[1]Physics Department, Space Science Center, University of New Hampshire, Durham, New Hampshire, USA, [2]Department of Atmospheric, Oceanic and Space Sciences, University of Michigan, Ann Arbor, Michigan, USA, [3]The Aerospace Corporation, Los Angeles, California, USA, [4]Department of Nuclear Engineering, University of Tennessee, Knoxville, Knoxville, Tennessee, USA, [5]Harvard-Smithsonian Center for Astrophysics, Cambridge, Massachusetts, USA, [6]Johnson Space Center, NASA, Houston, Texas, USA, [7]Southwest Research Institute, Boulder, Colorado, USA

Abstract We expand upon the efforts of Joyce et al. (2013), who computed the modulation potential at the Moon using measurements from the Cosmic Ray Telescope for the Effects of Radiation (CRaTER) instrument on the Lunar Reconnaissance Orbiter (LRO) spacecraft along with data products from the Earth-Moon-Mars Radiation Environment Module (EMMREM). Using the computed modulation potential, we calculate galactic cosmic ray (GCR) dose and dose equivalent rates in the Earth and Mars atmospheres for various altitudes over the course of the LRO mission. While we cannot validate these predictions by directly comparable measurement, we find that our results conform to expectations and are in good agreement with the nearest available measurements and therefore may be used as reasonable estimates for use in efforts in risk assessment in the planning of future space missions as well as in the study of GCRs. PREDICCS (Predictions of radiation from REleASE, EMMREM, and Data Incorporating the CRaTER, COSTEP, and other solar energetic particles measurements) is an online system designed to provide the scientific community with a comprehensive resource on the radiation environments of the inner heliosphere. The data products shown here will be incorporated into PREDICCS in order to further this effort and daily updates will be made available on the PREDICCS website (http://prediccs.sr.unh.edu).

1. Introduction

In the planning of manned missions, radiation in the form of galactic cosmic rays is a vital consideration in order to ensure the safety of personnel on the spacecraft as well as to prevent instrument failures. The goal of the Cosmic Ray Telescope for the Effects of Radiation (CRaTER) mission is to provide a characterization of the lunar radiation environment through the measurement of charged particles in excess of 10 MeV. The CRaTER telescope is comprised of three pairs of thin and thick silicon detectors which measure the energy deposited in them by energetic particles. The telescope is aligned perpendicular to the lunar surface with one detector pair facing zenith, one facing nadir, and one in the middle. The measured energy deposited can be divided by the path length of the radiation to obtain the lineal energy transfer (LET), with the thin detectors sensitive to high LET and the thick to low LET. By combining the detector pairs, one can get a picture of the entire LET spectrum. The deposited energy can also be used to compute dose rates. In this study, when we reference the CRaTER dose rate, we are referring to the combined D1-D2 zenith-facing detector pair dose rate which is calculated using methods described by *Schwadron et al.* [2012]. A thorough overview of the CRaTER instrument is provided by *Spence et al.* [2010].

In a companion paper, *Joyce et al.* [2013] showed that the Predictions of radiation from REleASE, Earth-Moon-Mars Radiation Environment Module (EMMREM), and Data Incorporating the CRaTER, Comprehensive Suprathermal and Energetic Particle Analyzer (COSTEP), and other solar energetic particles (SEP) measurements (PREDICCS) radiation system was capable of accurately modeling dose rates and accumulated dose using comparisons to the CRaTER instrument aboard the Lunar Reconnaissance Orbiter (LRO) spacecraft during three major solar energetic particle (SEP) events in 2012. In addition, that study used CRaTER measurements of galactic cosmic ray radiation together with data products generated by the EMMREM radiation model to compute the modulation potential at the Moon during the entirety of the LRO mission. That study demonstrated that due to the limitations of EMMREM, PREDICCS does a poor job modeling galactic cosmic ray (GCR) dose rates, and suggested that the computed modulation potential could

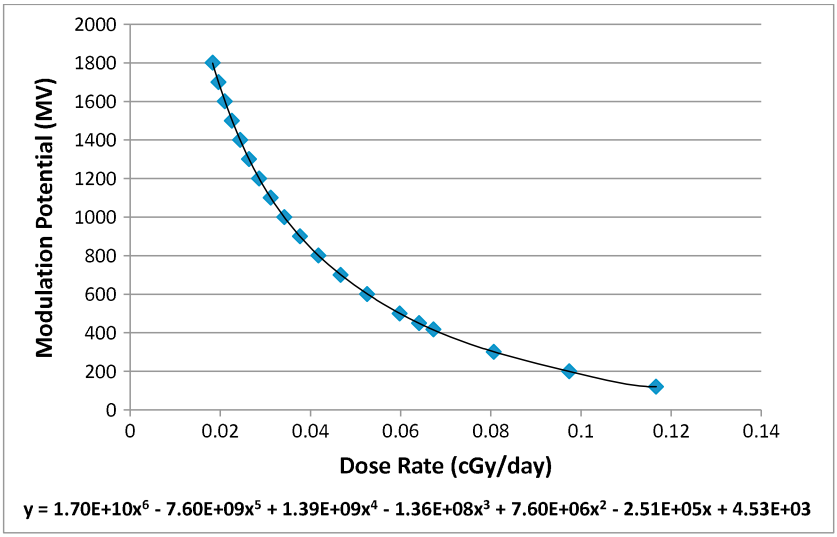

Figure 1. Plot of modulation potential versus GCR dose rate for atmospheric density of 0.0 g/cm^2 and shielding of 0.3 g/cm^2 (emulating lunar conditions). The data are taken from a lookup table based on the Badhwar-O'Neil model from *O'Neill* [2006] and are fit with a sixth-order polynomial in order to obtain an expression for modulation potential as a function of GCR dose rate. Plot originally from *Joyce et al.* [2013].

be used to compensate for this effect during times when the dose rate is not dominated by SEPs. Here, we expand upon those efforts by using the modulation potential to compute dose rates and dose equivalent rates at various altitudes in the Earth and Mars atmospheres. These methods will, in the future, be incorporated into the PREDICCS system, providing the scientific community with a tool for risk assessment in the planning of future missions and for use in the study of galactic cosmic rays.

2. Overview of Modulation Potential Calculation

Galactic cosmic rays are high-energy particles originating from outside our solar system which stream through the heliosphere. Due to the relatively low variability of their sources, GCRs are a constant presence in interplanetary space. As a result of the influence of the interplanetary magnetic field, GCRs lose energy as they stream through the heliosphere and the approximate amount of energy lost per unit charge is called the modulation potential. This quantity varies with the solar cycle, being greatest during solar maximum when elevated magnetic field strengths and heightened frequencies of coronal mass ejections pose greater obstacles to incoming GCRs. Because the modulation potential represents the energy lost by GCRs as they stream through the heliosphere, it is possible to infer the modulation potential at a point in space from the GCR dose rate at that location. Using the same modulation potential for all ion species and energies is a common approximation which yields reasonable results. The modeling done here is based on the model described by *O'Neill* [2006] which propagates the local interstellar energy spectrum through the heliosphere using the Fokker-Planck equation. This model is an update of the original model laid out by *Badhwar and O'Neill* [1991].

Joyce et al. [2013] took the hourly CRaTER-measured D1D2 skin dose rate described in detail by *Schwadron et al.* [2012] and removed measurements where the dose rate rose significantly above the large-scale background rate (periods of high-SEP activity) in order to obtain an approximate GCR dose rate over the course of the LRO mission. Then, using EMMREM-generated lookup tables containing dose rate data for various modulation potentials as well as atmospheric and shielding densities they calculated the modulation potential at the Moon. Given the local modulation potential, these tables may be used to compute dose rates behind different levels of shielding and for different atmospheric densities on Mars. By plotting modulation potential against dose rate for an atmospheric density of 0 g/cm^2 (consistent with conditions on the Moon) and shielding thickness of 0.3 g/cm^2 (most consistent with shielding seen by CRaTER) and fitting the plot with a sixth-order polynomial, they obtained an expression for the modulation potential as a function of GCR dose rate (Figure 1). Using this expression with the CRaTER dose rates, they computed the modulation potential over time. It is important to note that unlike *Joyce et al.* [2013], we have the ability to modify

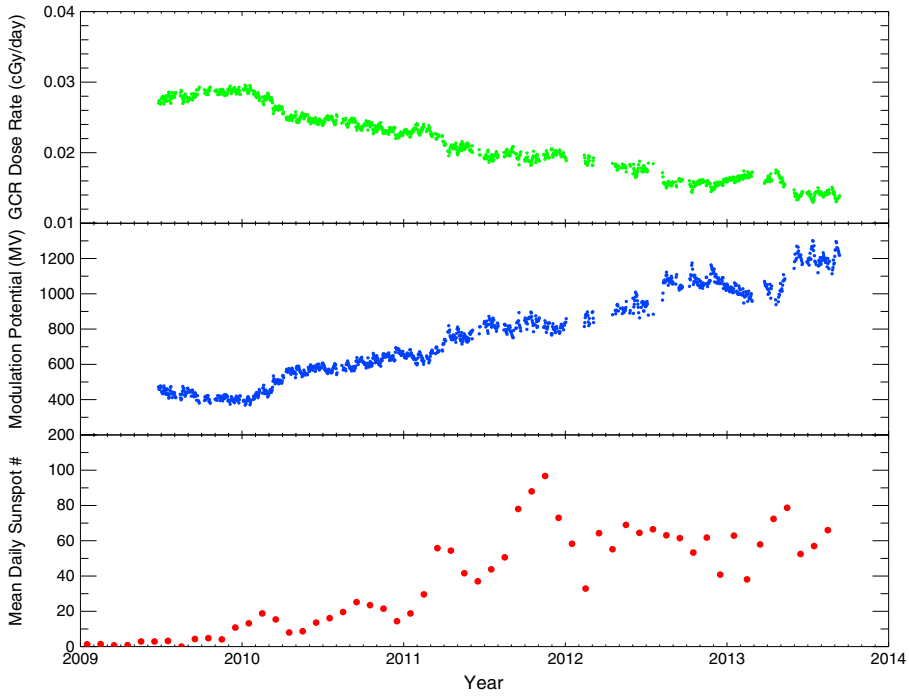

Figure 2. Plot of GCR dose rate and modulation potential at the Moon during the LRO mission as the Sun transitions from minimum to maximum. Sunspot number as provided by the Solar Influences Data Analysis Center (SIDC) is shown to provide context within the solar cycle. Plot has been updated from the one shown by *Joyce et al.* [2013].

the CRaTER GCR dose rate to remove the effect of secondary species coming from the Moon using results from *Spence et al.* [2013], which showed that these secondaries account for approximately 8.6% of the dose at LRO. We therefore reduce the dose rate by this amount in order to remove the effect of these secondaries which would not impact the dose rate in interplanetary space. Figure 2 shows the evolution of the modulation potential at the Moon over the course of the LRO mission. The mean monthly sunspot number according to the Solar Influences Data Analysis Center (available at http://sidc.oma.be/sunspot-data/) is also plotted in order to establish context within the solar cycle. We note that the exclusion of secondary species from the CRaTER dose rates results in a significant increase in the modulation potential compared to the *Joyce et al.* [2013] study, bringing the minimum values up to the 400–450 MV range typically associated with solar minimum. Using these values for the modulation potential, we can compute atmospheric dose and dose equivalent rates at Earth and Mars for various altitudes.

3. Computation of Atmospheric Dose Rate and Dose Equivalent Rate at Earth

We compute atmospheric dose and dose equivalent rates in Earth's atmosphere using a program based on the Badhwar-O'Neill model of *O'Neill* [2006], which describes the diffusion of GCRs through the heliosphere. The program takes a modulation potential as input and outputs an energy spectrum for a selected ion species. We then use dose lookup tables that contains dose/fluence values for various ion species, particle energies, and atmospheric densities (which correspond to different altitudes in the atmosphere from 11 to 36 km) to calculate dose rates. Each dose rate is computed through aluminum shielding of 1.0 g/cm^2, for a water depth of 1.0 cm which is a proxy for skin and eye, and assumes 2π exposure, meaning that half of the sky is blocked. For the sake of comparison, each computed dose and dose equivalent rate shown here is calculated using these same shielding, material, and exposure values, although we note that the CRaTER dose rate shown differs in shielding (0.22 g/cm^2). We also note that these tables are computed for the polar regions where the Earth's magnetic field has a minimal effect. Dose rates in other regions where the magnetic field is more important can be computed by using energy spectra which have been modified by the effect of the magnetic field. For each daily modulation potential value, we compute energy spectra for each of the available ion species. We can determine the dose rate contribution of a given ion species at a given energy by taking the corresponding flux value from the energy spectrum and multiplying it by the corresponding dose/fluence value from the lookup table to get a dose rate. By summing these values over

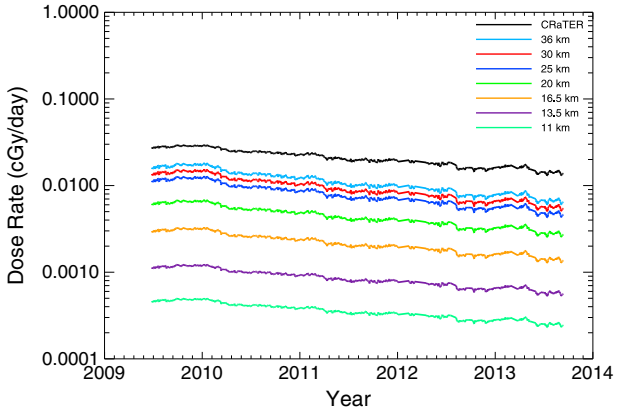

Figure 3. Plot of GCR dose rates in Earth's atmosphere for various altitudes, computed using the Badhwar-O'Neil model from *O'Neill* [2006] with EMMREM data products. The CRaTER dose rate is shown for the purpose of comparison, and as expected it somewhat exceeds the highest-altitude Earth dose rate. The Earth dose rates are computed behind 1.0 g/cm^2 shielding, while CRaTER is shielded by approximately 0.22 g/cm^2 aluminum shielding. We see that the dose rate at 36 km is approximately 34 times larger than at 11 km in 2009 during the extended solar minimum. This ratio decreases during the progression to solar maximum, falling to approximately 26 in 2013.

each species and energy separately for each altitude value we obtain the total GCR dose rate for different altitudes in Earth's atmosphere. As an additional point of reference for the reader, we studied the computed energy spectrum of protons using a typical solar minimum modulation potential of 450 MeV. Using the dose tables to compute dose rates for the highest available altitude (36 km), we found that ~95% of the dose is accounted for by protons in the energy range from 100 MeV to 10 GeV, with protons at approximately 1 GeV contributing the most.

Due to the time intensive nature of the Monte Carlo codes used to generate these tables, calculations have not been extended to the lower altitudes for all of the heavier ion species. Therefore, the dose rates for the highest three altitudes (25, 30, and 36 km) are computed using ions of atomic number 1 through 25 as well as 28, where the lower altitudes (11, 13.5, 16.5, and 20 km) are computed using only ions of atomic numbers 1 through 8. Due to the relatively low flux of the heavier ions, the effect this has on the lower altitude dose rates should be negligible, and in fact, when we compute the dose rate for the higher altitudes using only the lighter ions ($z = 1$–8) we see a decrease of only approximately 0.2% relative to the same dose rates computed with the heavier ions included, and we see no reason for a larger discrepancy at lower altitudes.

Figure 3 shows the evolution of the computed GCR dose rate at different altitudes in Earth's atmosphere over the course of the LRO mission. The CRaTER dose rate is shown for comparison and as expected it is somewhat greater than the highest-altitude Earth dose rate since there is no atmosphere at the Moon to pose as a shield for the GCRs. We observe that the highest-altitude rate exceeds the lowest by a factor of approximately 34 at the outset of the mission and drops to a factor of 26 greater by the most recent measurements.

Dose equivalent is a quantity of dose which is somewhat more useful in determining the danger radiation poses to humans and is weighted by a quality factor based on the biological damage potential of the incident radiation. The quality factor depends on the LET of the radiation and this functional dependence is shown in Table 1. In order to compute dose equivalent rates in Earth's atmosphere, we use an EMMREM lookup table containing LET values for the same ion species, particle energies, and atmospheric densities used in the dose rate calculations to compute the quality factors necessary to compute the equivalent dose rates. Figure 4 shows the evolution of the computed GCR dose equivalent rate over the course of the LRO mission. Additionally, we plot the ratio of the dose equivalent rates to the dose rates for each altitude, yielding the dose-weighted average of the quality factor (<Q>). We observe little to no difference between the dose and dose equivalent rate for any of the altitudes except for the highest altitude where we see an increase of approximately 7–8% to the dose rate.

Table 1. Quality Factor for Converting Dose to Equivalent Dose as a Function of LET in Water as Specified by the International Commission on Radiological Protection, Report 103 [*ICRP*, 2007]

Lineal Energy Transfer (keV/μm)	Quality Factor
LET < 10	1
10 ≤ LET ≤ 100	0.32 LET −2.2
LET > 100	$300/\sqrt{\text{LET}}$

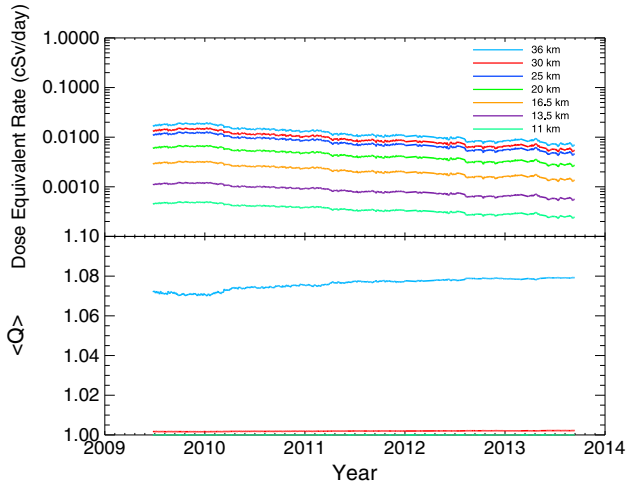

Figure 4. Plot of the computed GCR dose equivalent rate for various altitudes in Earth's atmosphere over the course of the LRO mission. These dose equivalent rates are computed by multiplying the dose rates shown in Figure 3 by the quality factor shown in Table 1. Also shown is the ratio between the dose and dose equivalent rates, which gives the dose-weighted quality factor <Q>. We see that there is little to no difference between the dose and dose equivalent rates except for at the highest altitude where we see an approximate 7–8% increase relative to the dose rate.

This result can be understood upon examining the LET tables used to compute the quality factor. Based on Table 1, we see that for there to be a difference between the dose and dose equivalent rates the LET must exceed 10 keV/μm. By scanning the lookup tables, we see that this threshold is only exceeded by certain heavy ions and only at the very highest altitudes. The reason for this is that the heavy ions which have LET high enough to push the quality factor above one have relatively low penetration depths and are quickly broken up by the atmosphere into lighter secondary particles which have much lower LET, and thus, the dose contribution at lower altitudes of incident heavy ions are not weighted more heavily by the quality factor.

4. Computation of Atmospheric Dose and Dose Equivalent Rates at Mars

We now calculate dose rates in the Martian atmosphere by scaling the computed modulation potential out to Mars and reversing the process used to calculate the modulation potential in order to obtain GCR dose rates. Using theory from *O'Neill* [2006], *Schwadron et al.* [2010] show that the modulation potential can be scaled to different locations in the heliosphere according to

$$\Phi(r,t) = \Phi_1(t)\frac{\arctan(R_b/r_0) - \arctan(r/r_0)}{\arctan(R_b/r_0) - \arctan(r_1/r_0)} \quad (1)$$

where Φ is the modulation potential at a distance r outward from the Sun, Φ_1 is the reference modulation potential at r_1, R_b is the distance to the outer modulation boundary (taken to be 100 AU), and r_0 is 4 AU. Using the modulation potential measured by CRaTER at the Moon (1 AU) as reference, we compute the modulation potential at Mars (1.5 AU).

Having obtained the modulation potential, we use the same lookup table used to generate Figure 1 and reverse the process, plotting dose rate against modulation potential for various atmospheric densities and fitting the plots to obtain expressions for GCR dose rate as a function of modulation potential. Then, using the modulation potential at Mars, we use these expressions to calculate dose rates for various atmospheric densities behind aluminum shielding of 1.0 g/cm^2. Because altitude is a more meaningful quantity than atmospheric density in this case, we use the conversions shown in *Townsend et al.* [2013] to express the dose rate at different altitudes in the Martian atmosphere. Figure 5 shows the evolution of these dose rates over the course of the LRO mission. We see that the 30 km altitude dose rate at Mars is somewhat larger than the CRaTER dose rate, reflecting the fact that since the GCRs have traveled a shorter distance through the heliosphere, they have lost less energy and contribute a greater dose. The 30 km Mars dose rates are larger than the Earth dose rates by a factor of 2–2.5 due to a combination of the above effect as well as the reduced atmospheric density. The plot also shows that, due to the relatively low atmospheric densities, there is less

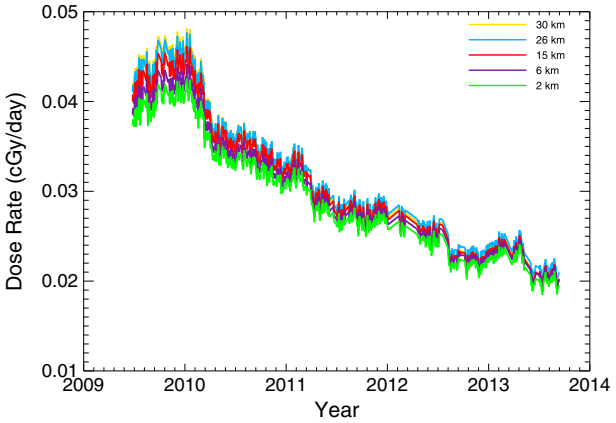

Figure 5. Plot of GCR dose rates in the Martian atmosphere for various altitudes. The dose rates are calculated by scaling the modulation potential out to Mars and reversing the process used to compute the modulation potential to obtain dose rates. We see that as expected the Martian dose rates are higher than those for the Earth due to the relatively low atmospheric density as well as the fact that the GCRs have lost less energy over a shorter distance into the heliosphere. We also observe that, due to the relatively low density of the Martian atmosphere, there is a much smaller difference between dose rates at different altitudes, varying by approximately 9% at the beginning and 6% at the end.

variation between the different altitudes, with the highest altitudes exceeding the lowest by only 9% at the outset of the measurements and decreasing to 6% by the most recent measurements.

Zeitlin et al. [2013] reported GCR dose rates measured by the Mars Science Laboratory (MSL) en route to Mars of 0.048 cGy/d. This dose rate was measured in silicon, then converted to water and averaged over measurements taken from 6 December 2011 to 14 July 2012 during transit to Mars. Because these measurements took place in free space, where our computed rates assume the sky is half blocked by Mars, the actual rate we should compare to is 0.024 cGy/d. This is comparable, though somewhat smaller than our computed rates which, for the highest altitude, are around 0.03 cGy/d during the same time period. The most likely explanation for this discrepancy is that the GCR dose rate increases radially outward from the Sun, and since MSL was in transit to and had not landed on Mars during these measurements, it would see a lower average rate. Therefore, the observed discrepancy is reasonable and this comparison lends credibility to our calculations.

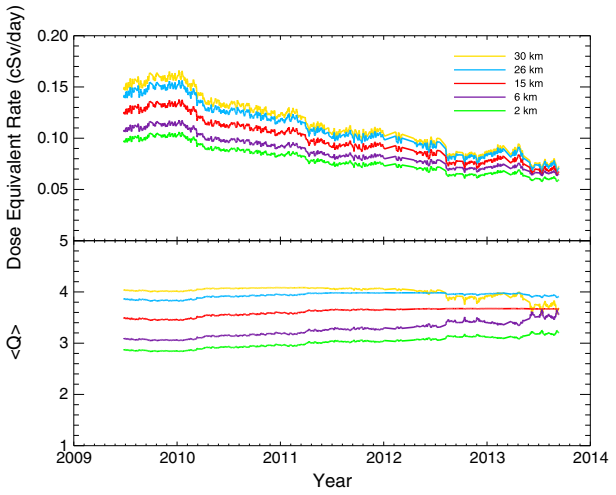

Figure 6. Plot of GCR dose equivalent rates in the Martian atmosphere for various altitudes as well as the dose-weighted quality factor <Q>. These are computed much in the same way as the Martian dose rates using dose equivalent lookup tables. We see that, unlike for Earth, the dose equivalent rate values differ significantly from the dose rate values, being approximately a factor of 4 greater for the highest altitude and 3 for the lowest. We also see greater variation among the dose equivalent rates for different altitudes with the highest altitude being greater than the lowest by approximately 53% initially and 22% most recently.

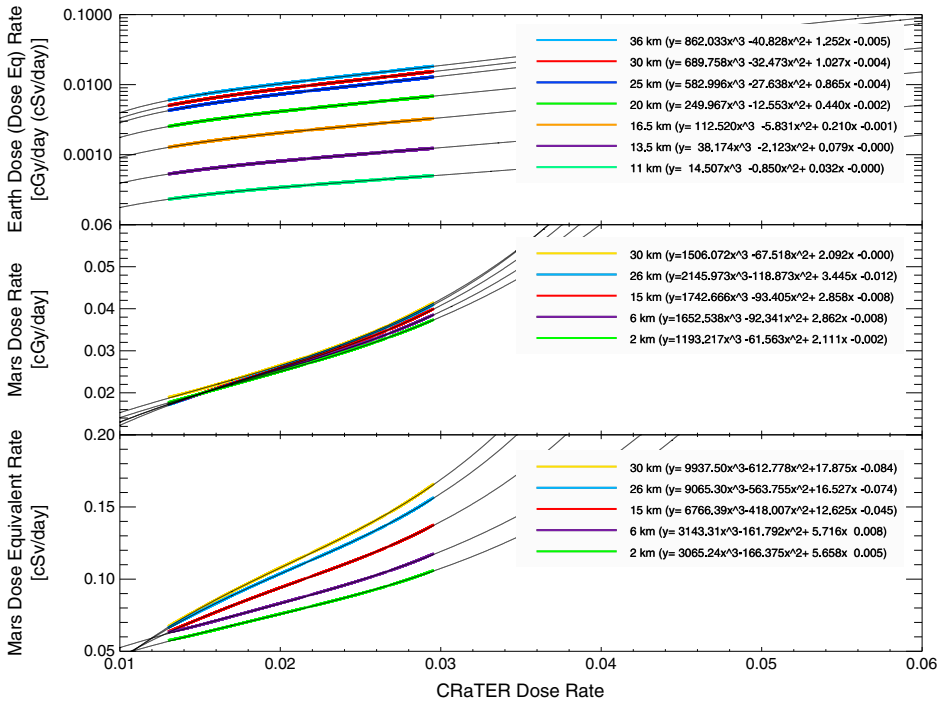

Figure 7. Plot of computed dose and dose equivalent rates for varying altitudes in the Earth and Mars atmospheres. Each curve is well described by a third-order polynomial fit. The functional forms are provided to enable future studies to easily estimate atmospheric dose rates during times when CRaTER data are unavailable using measurements or estimations of the dose rate at 1 AU through a similar level of shielding.

To compute dose equivalent rates in the Martian atmosphere, we apply the same process as for dose rates instead using lookup tables containing dose equivalent rates as a function of modulation potential. Figure 6 shows the resulting dose equivalent rates in the Martian atmosphere for various altitudes over the course of the LRO mission as well as the dose-weighted quality factor. We see that unlike for Earth, there is a significant increase of approximately a factor of 4 of the dose equivalent rates relative to the dose rates for the highest altitude and 3 for the lowest. The plot also shows a greater variation in dose equivalent rate for different altitudes, with the highest altitude being greater than the lowest by 53% at the beginning and 22% by the end of the measurements. This results from the fact that, as previously discussed, heavier ions contribute much more to the dose equivalent than lighter ions and since they are fragmented at higher altitudes, the dose equivalent rates at lower altitudes will decrease relative to higher altitudes more than the dose rates.

5. Summary

We have expanded upon the efforts of *Joyce et al.* [2013], using the modulation potential derived there to compute dose and dose equivalent rates for various altitudes in the Earth and Mars atmospheres. The results we obtain conform to expectations and are comparable to the nearest measurements available and may therefore reasonably be used as estimations in the planning of future space missions, as well as in other fields of study. Currently, preparations are being made to set up the engineering model of the CRaTER instrument to begin taking measurements either on the ground or possibly in orbit around the Earth. These measurements could provide an additional means of testing the validity of the calculations shown here.

Table 2. Second Order Polynomial Fit Functions of Dose Rates for Various Levels of Shielding for an Atmosphere of 0 g/cm^2[a]

Shielding (g/cm^2)	Fit Function
0.0	$y = -0.679x^2 + 0.705x - 1.52E\text{-}04$
1.0	$y = -0.330x^2 + 1.029x - 8.59E\text{-}05$
5.0	$y = -1.124x^2 + 1.071x + 8.27E\text{-}05$
10.0	$y = -1.583x^2 + 1.079x + 4.30E\text{-}04$

[a]The four levels of shielding shown correspond to (in increasing order) no shielding, thick spacesuit, spacecraft, and thick spacecraft. These dose rates are given as a function of the dose rate for a normal spacesuit (0.3 g/cm^2) which is closest to the shielding for CRaTER. These functional forms are given to provide readers with an easy means of converting dose rates between different levels of shielding.

Figure 7 shows the relationship between the measured CRaTER dose rate and the computed dose and dose equivalent rates in the Earth and Mars atmospheres. The computed rates are plotted against the CRaTER dose rate and are found to be well described by a third-order polynomial fit over the range of measurements. The functional forms of these fits are provided so that future studies may be able to easily estimate atmospheric dose and dose equivalent rates for times when CRaTER data are unavailable (either prior to being launched or once it is no longer online), using dose rate measurements or estimations at 1 AU using similar levels of shielding. Additionally, Table 2 shows the functional dependence of dose rates for different levels of shielding as a function of the dose rate most analogous to CRaTER. These dose rates are taken from the EMMREM-generated table mentioned previously, with each dose rate taken for 0 g/cm^2 atmosphere and given as a function of the dose rate for 0.3 g/cm^2 shielding. These are provided to allow easy conversions between different levels of shielding. The data products shown here will soon be incorporated into the PREDICCS radiation system and made available to the scientific community as a tool for use in the study of GCRs and for efforts in risk assessment in future missions.

Acknowledgments
Thanks to everyone on the CRaTER team for their help and guidance. This work is supported by NASA LRO/CRaTER/PREDICCS Project (contract NNG11PA03C), the NSF/FESD Sun-to-Ice Project (grant AGS1135432), and the NASA/LWS/NSF EMMREM Project (grant NNX11AC06G).

References

Badhwar, G. D., and P. M. O'Neill (1991), An improved model of galactic cosmic radiation for space exploration missions, *Int. J. Radiat. Appl. Instrum. Part D*, *20*(3), 403–410.

ICRP (2007), The 2007 Recommendations of the International Commission on Radiological Protection, ICRP Publication 103, *Ann. ICRP*, *37*(2–4), 1–332.

Joyce, C. J., et al. (2013), Validation of PREDICCS using LRO/CRaTER observations during three major solar events in 2012, *Space Weather*, *11*, 350–360, doi:10.1002/swe.20059.

O'Neill, P. M. (2006), Badhwar O'Neill galactic cosmic ray model update based on advanced composition explorer (ACE) energy spectra from 1997 to present, *Adv. Space Res.*, *37*, 1727–1733, doi:10.1016/j.asr.2005.02.001.

Schwadron, N. A., et al. (2010), Earth-Moon-Mars Radiation Environment Module framework, *Space Weather*, *8*, S00E02, doi:10.1029/2009SW000523.

Schwadron, N. A., et al. (2012), Lunar radiation environment and space weathering from the Cosmic Ray Telescope for the Effects of Radiation (CRaTER), *J. Geophys. Res.*, *117*, E00H13, doi:10.1029/2011JE003978.

Spence, H. E., et al. (2010), CRaTER: The Cosmic Ray Telescope for the Effects of Radiation experiment on the Lunar Reconnaissance Orbiter mission, *Space Sci. Rev.*, *150*, 243–284, doi:10.1007/s11214-009-9584-8.

Spence, H. E., M. J. Golightly, C. J. Joyce, M. D. Looper, N. A. Schwadron, S. S. Smith, L. W. Townsend, J. Wilson, and C. Zeitlin (2013), Relative contributions of galactic cosmic rays and lunar proton "albedo" to dose and dose rates near the Moon, *Space Weather*, *11*, 643–650, doi:10.1002/2013SW000995.

Townsend, L. W., J. A. Anderson, A. M. Adamczyk, and C. M. Werneth (2013), Estimates of Carrington-class solar particle event radiation exposures as a function of altitude in the atmosphere of Mars, *Acta Astronaut.*, *89*, 189–194, doi:10.1016/j.actaastro.2013.04.010.

Zeitlin, C., et al. (2013), Measurements of energetic particle radiation in transit to Mars on the Mars Science Laboratory, *Science*, *340*, 1080–1084, doi:10.1126/science.1235989.